한국지반공학회 연약지반처리위원회 '2000 학술발표회 / Feb. 18, 2000 / Seul, Korea

콘 관입시험을 이용한 연약지반 압밀특성 평가

Determination of Consolidation Characteristics in Fine Soils Evaluated by Piezocone Tests

임병석, Beyong-Seock Lim

고려대학교 부설 방재과학기술연구센터 선임연구원, Senior Researcher, Research Center for Disaster Prevention Science and Technology, Korea University.

SYNOPSIS : 본 연구의 목적은 연약지반의 압밀계수 측정에 있어 Piezocone 관입시험을 이용할 때 관입시험자체의 정확성과 시험결과들에 미치는 여러 가지 지반공학적 영향요소들을 고려하려는데 있다. 본 연구의 연구실험방법으로는, Piezocone 관입을 위한 연약모형지반 조성을 위하여 초대형 Slurry Consolidometer에 Free Stress 상태의 Slurry를 45일간 압밀시킨 후 Automatic Computer Control Calibration Chamber (LSU/CALCHAS; Louisiana State University Calibration Chamber System)에 옮긴후 다시한번 압밀시키는 Two-Stage Consolidation Method를 사용하였다 동시에 연약모형지반내에 8개의 Piezometer를 설치하여 Piezocone 관입시 유발되는 지반 내에서의 과잉간극수압의 변환을 측정하였다. 총 25개의 Piezocone 시험중 4개는 Standard 10cm^2 Piezocone이고, 나머지 21개는 Miniature Piezocone이 사용되었다. 모형지반은 여러 가지 Boundary Condition들과 Stress Condition 그리고 Stress History등을 고려하여 조성되었다. 또한 Dissipation Test직후의 압밀특성을 확인하기 위하여 0.01초당 한 개이상의 실측점을 측정할 수 있는 Digital-Oscilloscope를 이용하였다. 특히 Dissipation Test, 즉시 Piezocone의 Filter Element에 잡히지 않는 과잉간극수압의 Initial Drop 존재에 관한 기존의 추측을 실제 실험치로 확인할 수 있었다.

Key Words : Piezocone, Calibration Chamber, Dissipation Test, Initial Drop

1. INTRODUCTION

Estimation of consolidation and flow characteristics in fine grained soils has received much attention in modern soil mechanics. The primary consolidation parameters considered are the coefficient of consolidation and the hydraulic conductivity for settlement and seepage analysis. Consolidation parameters are usually estimated from oedometer tests or back analyses of field performance. In spite of their popularity, the oedometer tests and back analysis have some limitations in the determination of consolidation and permeability parameters.

Lately, there has been an increasing trend to use the piezocone penetration test (PCPT) as an in situ tool of choice for determining the consolidation and flow characteristics of cohesive soils. However, the current interpretation of consolidation and flow characteristics using piezocone test has not been entirely satisfactory to eliminate a number of pressing needs in design and testing practice.

A satisfactory interpretation of PCPT requires precisely controlled field and laboratory calibration tests. Field calibration of the piezocone has numerous limitations and flaws due to soil inhomogeneities and uncertainties regarding the magnitude of in-situ stresses and stress history of the deposit. The use of laboratory calibration chamber to calibrate an in-situ device has definite

advantages since homogeneous, reproducible and instrumented soil specimens, subjected to a known stress history can be prepared and tested under controlled boundary conditions.

Laboratory calibration chamber tests for cone pentrometers, pressuremeters and dilatometers in cohesionless soil specimens have been conducted by numerous researchers. However, there have been only few applications to compacted or preconsolidated cohesive soils. This can be attributed to the extremely time consuming and laborious process involved in the preparation of large cohesive soil specimens in addition to other complexities involving instrumentation for pore pressure monitoring and the need for maintaining saturation by back pressure.

This research presents results of four standard 10 cm2 piezocone penetration tests, twenty one miniature piezocone penetration tests on large instrumented cohesive soil specimens in a calibration chamber system. By using a two-stage slurry consolidation technique, cohesive soil specimens of very high quality were obtained. The time consuming and laborious soil sample preparation limited the number of tests that were conducted. Mainly, the performance of the piezocone penetrometer to predict consolidation and flow characteristics are evaluated.

2. BACKGROUND

The pore pressure measured by piezocone can be divided into two components:
- in situ hydrostatic pressure (u_0)
- excess pore pressure generated by piezocone intrusion ($\triangle u$)

The excess pore pressure($\triangle u$) is a combination of two different stresses : octahedral excess pore pressure ($\triangle u_{oct}$) and shear-induced excess pore pressure ($\triangle u_{shear}$), such that

$$\triangle u = \triangle u_{oct} + \triangle u_{shear}$$

According to Campanella et al (1988), when saturated soils are subjected to an increase in octahedral stresses, positive pore pressures are generated. When subjected to only shear stresses, pore pressures generated can be either positive or negative depending on the contractive or dilative response of the soil to shear. The time variation of the excess pore pressure provides information concerning the coefficient of consolidation. To evaluate the dissipation of the excess pore pressure, piezocone is stopped and the decay of pore pressure ($\triangle u$) with time is recorded. Typical dissipation curves for soft clay plotted on a logarithmic scale is shown in Figure 2.1 The excess pore pressure can be defined as :

$$\Delta u_p = u_p - u_0$$

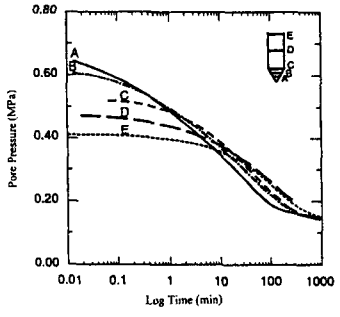

Figure 2.1 Typical dissipation test results (Lunne et. al., 1997)

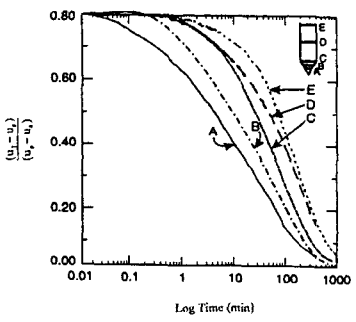

Figure 2.2 Normalized dissipation tests curves. (Lunne et. al., 1997)

u_p is the measured total excess pore pressure at the time of penetration arrest and u_0 is the in-situ hydrostatic pressure. Interpretation of dissipation records is generally based on a normalized excess pore pressure ratio U, defined as:

$$U = \frac{\Delta u}{\Delta u_p} = \frac{(u_T - u_0)}{(u_p - u_0)}$$

Where Δu is the excess pore pressure at the depth of interest changing with time in dissipation tests, Δu_p is the penetration excess pore pressure at the time of penetration arrest and Δu_T is the total excess pore pressure at any time t. Figure 2.1 can be replotted in normalized form as Figure 2.2 Generally, piezocone penetration involves both vertical and horizontal drainage. For porous elements located behind the tip, the drain flow is governed predominantly by radial (horizontal) direction. For radial drainage, the differential equation of Terzaghi (1925) and Rendulics (1935) consolidation theory is expressed as

$$\frac{\partial u}{\partial t} = c_r\left(\frac{\partial^2 u}{\partial r} + \frac{1}{r}\frac{\partial u}{\partial r}\right)$$

where u = excess pore pressure, r = radial distance from the centerline of the piezocone, t = time (t = 0 at arrest of piezocone), c_r = coefficient of consolidation in radial direction (T x r^2 / t), and T = nondimensional time factor. This differential equation is valid for an axisymmetrical condition with no vertical drainage of the soil during dissipation test. Piezocone penetration generates excess pore pressure around the probe in normally consolidated cohesive soils, which reduce the effective stresses in the surrounding soils. This indicates unloading stage.

However, during dissipation of excess pore pressure the effective stresses surrounding piezocone increases, which indicates that the stress state of soil is under reloading state, (the overconsolidated , OC, state). As dissipation continues, the increasing effective stresses exceed the reloading state and enter into the normally consolidated (NC) loading state. The degree of dissipation shorter than the 50% ($U_{0.5}$) is generally assumed as the effective stress around piezocone under the reloading state. Hence, the recording of the dissipation results should continue until at least half the initial excess pore pressure has dissipated (U=0.5). However, the above explanation is based on Terzaghi (1925) & Rendulic (1935) uncoupled consolidation theory. If the effect of coupled consolidation is taken into account, the total stress is not constant with the increase of generated excess pore pressure during penetration. It is hard to estimate how much effective stress interacts with the variation of excess pore pressure.

2.1 INTERPRETATION METHOD

The accuracy with which the coefficient of consolidation characteristics are determined will depend on the interpretation method adopted. Many investigators have proposed various interpretation methods for analyzing the consolidation that occurs when piezocone penetration is stopped. They can be classified as:

. Cavity expansion models
. Strain path method
. Semi-empirical method
. Finite element analysis

2.2 Excess Pore Pressure Drop Due to Normal Stress Release

The excess pore pressure drop due to normal stress release when a cone penetrometer is stopped has not been given proper attention, because this feature is not easily identified in field tests due to soil inhomogeneities. If this initial drop of excess pore pressure is ignored, the interpretation of dissipation results can not be achieved correctly. It was recommended (Kurup, 1993 ; Kurup et al, 1994; Voyiadjis et al, 1994; Kurup et al, 1995) that the interpretation of the dissipation results to evaluate the coefficient of consolidation should be based on the initial dissipation values of excess pore pressure u_i, and not the penetration excess pore pressure, u_p.

This initial, drop which is primarily due to the normal stress reduction that occurs when penetration ceases, is influenced by a variety of factors such as the rate of penetration, stress-strain behavior at very high strain rates, OCR, K_0, plasticity index and hydraulic conductivity. Improper clamping of the penetrometer rod, and filter expansion (flexible filters) due to normal stress reduction at the tip, are other factors that can contribute to the sudden drop in excess pore pressures (Kurup & Tumay, 1995). Monitoring tip resistance during dissipation tests can provide further information regarding this normal stress reduction. There are essentially two effects that influence the cone resistance and excess pore pressure during varying rates of penetration, (1) Viscous and dynamic effects, and (2) Drainage effect. The effect of rate the of penetration on cone resistance and generated pore pressures and drop in their values when penetration is stopped for a dissipation analysis, need to be investigated for a proper interpretation of the coefficient of radial consolidation. The penetration rate changes abruptly from 2 cm/s to 0 cm/s when the cone is stopped for a dissipation test, resulting in a steep decrease in cone resistance accompanied by a sudden drop in the excess pore pressures at the tip. This influence of penetration rate on excess pore pressure should be considered by a coupled (between total stresses and pore pressure) consolidation analysis taking into account the dissipation that occurs even during penetration.

3. DESCRIPTION OF THE TESTING EQUIPMENT

3.1 CONE PENETROMETERS

Two kinds of cone penetrometers were used in this study (Figure 3.1). They are :

(1) Miniature piezocone (piezocone, piezo/friction cone)

(2) Standard 10 cm2 piezocone (Reference cone)

3.1.1 MINIATURE PIEZOCONE

Two kinds of miniature piezocones were utilized for this research. A schematic view is shown in Figure 3.1. Both piezocones are equipped to measure cone (tip) resistance. One has no friction sleeve, the other has a sleeve 43 mm long friction sleeve behind cone base. The latter type (piezo/fricition cone) push rod has a reduced diameter 9.53 mm compared to the friction sleeve which is a 11.28 mm in diameter. Piezo/friction cone has its own preamplifier housed in the connector which routes tip resistance, friction resistance and pore pressure signals to the Data

Acquisition System. The miniature piezocone (no friction sleeve) needs a separate amplifier to connect to the Data Acquisition System. This cone is also fully compatible with the standard instrumentation equipment of the reference cone penetrometer. Miniature piezocone (no friction sleeve) penetrometer used in this study was manufactured by Fugro Geosciences, Inc., Houston, TX, U.S.A. The manufacturer of piezo/friction cone was Fugro-McClelland Engineers B.V., The Netherlands. Both miniature piezocones have a projected cone area

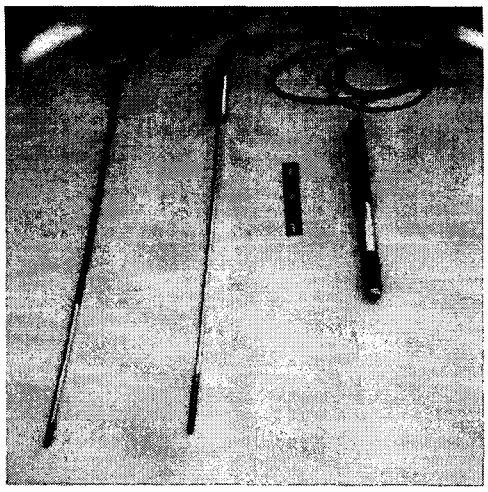

Figure 3.1 Cone Penetrometers (mini-piezocone, mini-piezo/friction cone, and reference cone)

of 100 mm2 and a cone apex angle of 600. The maximum normal load capacity is 5 KN. The filter location can be changed from u_1 configuration (the lowest ¼ of the cone at the very tip) to u_2 configuration (0.5 mm above the base of the cone and 2 mm vertical height). The maximum pore water pressure transducer capacity is 3.5 Mpa. The area ratio (λ) for the correction of measured cone resistance, q_c, of miniature piezocone is 0.62.

3.1.2 REFERENCE CONE

The Reference quasi-static electric cone penetrometer (RQSEC) is a standard 35.6 mm nominal diameter Fugro piezocone penetrometer (Figure 3.1). This cone is generally accepted as a standard cone penetrometer in the United States and in Europe. It has a 10 cm^2 cone tip (35.6 mm in diameter) with an cone apex angle of 60^0. It has also a friction sleeve base with a surface area of 150 cm^2 located behind cone and pore water pressure piezometric element located on cone face. The area ratio (λ) is 0.64. Therefore it can measure cone tip resistance, sleeve friction, and pore water pressure (u_1 at cone face) simultaneously.

3.2 SLURRY CONSOLIDOMETER

The slurry consolidometer system was designed by Dr. Pradeep U. Kurup (1993). The device is designed to produce uniform and repeatable cohesive samples which simulate naturally sedimented soils by consolidating a slurry under K_0 conditions. The consolidometer body consists of two PVC tubes, 525 mm inside diameter, 15 mm thick, and 812 mm high (Figure 3.2). It is split longitudinally into two halves and bolted together. The reason for split design is to avoid any mechanical extrusion, disturbance and man handling the specimen while transferring it into the

calibration chamber after consolidation. The inside surface of the lower tube is lined with sand paper to offer friction and avoid slippage of the membrane caused by the consolidating slurry. The two tubes, upper collar and lower split tube, are held together using six steel rods connecting an aluminum top lid to the bottom base frame. Four rollers support the base frame in order to move the whole consolidometer easily. Double drainage is allowed for the slurry to consolidate. For this drainage, a porous stone is attached to both the upper surface of the base plate and the bottom surface of the piston rod which provide vertical consolidation pressure to specimen.

3.2.1 LOADING SYSTEM

The consolidometer is designed to consolidate the specimen up to a maximum vertical stress of 552 Kpa. The consolidation pressure is furnished by a single acting hydraulic cylinder (push jack) with power provided by an air-hydraulic pump. This pressure is transferred through the push jack to a steel piston rod, an aluminum piston plate , and finally to the slurry specimen. The pump has an automatic pressure make-up feature. This feature enables it to keep a constant consolidation pressure until the end of consolidation. The pressure transducer is installed on a hub which connects the servo controlled air - hydraulic pump and the push jack in order to monitor by the computer the consolidation stress during consolidation. The vertical settlement of the slurry specimen is recorded by a linear varying displacement (LVDT) connected to the piston rod.

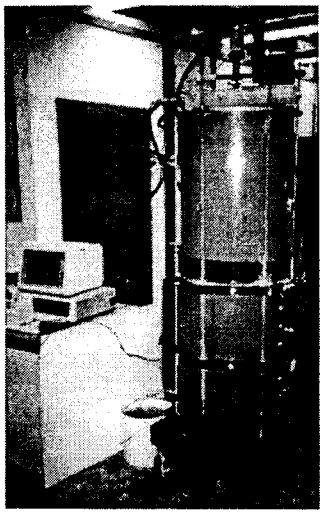

Figure 3.2 Slurry consolidometer (Kurup, 1993)

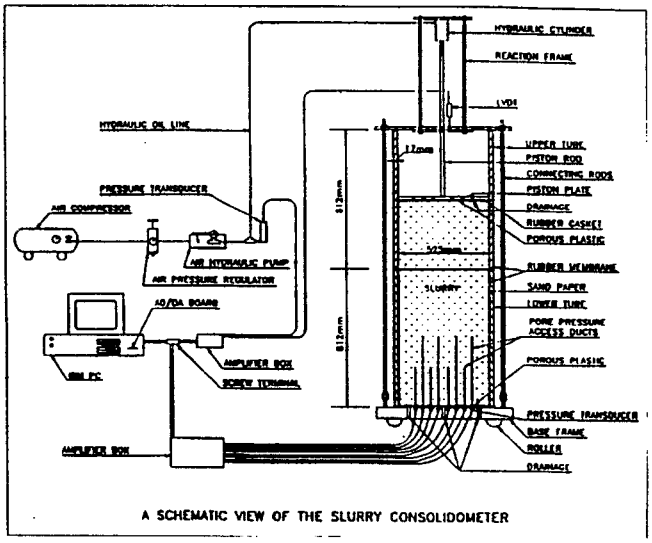

Figure 3.3 A schematic of view slurry consolidometer (Kurup, 1993)

3.2.2 INSTRUMENTATION

Miniature pore water pressure transducers are installed inside the slurry specimen. The leads for these instruments come through the bottom of the aluminum base plate, which has eight access holes at fixed positions. There are also three more access holes for drainage/back pressure in the base plate. The miniature pore pressure transducer consists of a stainless adapter, ducts consisting of stainless hypodermic needles with a 1.2 mm inside diameter and a thickness of 0.23 mm. The length of the ducts are designed to monitor pore water pressure at two different elevation and varying radial distances, above the base plate (Figure 3.3).

The tips of the ducts are sealed with a porous plastic filter material to prevent soil migration and clogging of the tubes. The other end of the tip is connected to the pressure transducer ports. The accuracy of pore pressure measurements depends on the response time and this in turn is mainly dependent upon the degree of saturation.

The miniature pressure transducers are saturated through a dual stage saturation technique to keep a high quality response time. In the first stage of saturation, the ducts attached to the adapter are saturated by flushing with de-aired water, using a special CPV 1000 closed circuit pump. The ducts with attached adapter are joined with the pressure transducer submerged in a tub of de-aired water. Secondly, the tips of the ducts are immersed in de-aired water and then subjected to vacuum in the Nold Deaerator. The response of the pore pressure transducer on initially pressurizing the slurry is instaneous and is equals to the applied pressure. The data acquisition software acquires and appends pore water pressure, consolidation stress, and settlement into a file and displays the data on computer screen in graphical form plotted in real time. A schematic view of the slurry consolidometer set up is shown in Figure 3.3.

3.3 The LSU CALIBRATION CHAMBER SYSTEM

The calibration chamber system LSU/CALCHAS was designed by Dario C. De Lima (1990) under the supervision of Dr. M.T. Tumay. The LSU/CALCHAS (Tumay and de Lima, 1992) consists of a calibration chamber, a panel of controls, a data acquisition and control system, a hydraulics and chucking system, and a penetration depth measurement system (Figure 3.6). This chamber allows testing of different size of cone penetrometers under controlled boundary conditions. The diameter ratio with respect to the miniature piezocone used in this investigation is 41, and the diameter ratio with respect to the reference cone is 15. The double wall chamber is flexible, and can house specimens 525mm in diameter and 815mm high. Its operation is servo-controlled and is capable of consolidating soil specimens at a variety of stress paths including Ko (zero lateral strain) consolidation.

The chamber is divided into two sections; namely the piston cell and the chamber cell unit (Figure 3.7). The chamber cell rests on a bottom plate of 640 mm in diameter and 38.1 mm in thickness. The piston pushes the bottom plate upwards thereby applying a vertical stress on the specimen. As shown Figure 3.7, the two cylindrical shells made of stainless steel 304 plates are 6.35 mm thick. The internal diameter of the inner and outer shells are 560 mm and 580 mm, respectively, and 910 mm high. The shells are designed to withstand a maximum pressure of 1440 kN/m^2.

The sample top and bottom plates are made of 6061 T-6 aluminum and are of 530 mm in diameter. The sample bottom plate rests on the piston cell unit. The sample top plate is bolted to the chamber top plate (top lid) which is 640 mm in diameter and 31.1 mm in height. The chamber can simulate the four traditional boundary conditions of stress and strains.

3.3.1 CONTROL PANEL

The control panel instruments used for regulating the operation of the chamber are grouped together within reach of the operator on a vertical wooden panel of 1.22 m 1.96 m. Copper tubing is used for all control lines to minimize volume changes and hence the compressibility in the system. Three quick-connectors link the three water pressure lines from the panel of controls to the piston and sample cells. A picture of panel is shown in Figure 3.6.

The main unit of the panel of controls have four components: pressure regulators, electro-pneumatic transducers, pressure transducers, pressure gauges. They consist of five Sen Sym ST2000 pressure transducers, four Marsh process gauges, two Fairchild back pressure regulator, and four Fairchild electro-pneumatic transducers. The electro-pneumatic transducer converts an electric signal to a linear pneumatic signal. A DC signal of 0 to 10 V is generated. Two of the transducers are used in the piston cell operation for applying the vertical stress to the sample. The other two are used for the pressure compensation between the sample inner and outer shells during K_0 consolidation and penetration phase. The panel is equipped with an air-water systems that apply the vertical and horizontal pressure, and saturate specimens under back pressure.

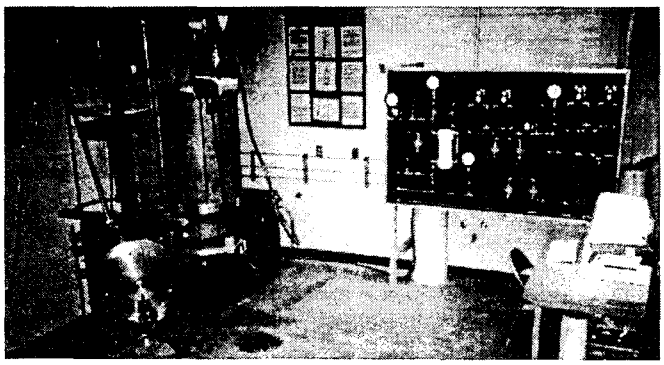

Figure 3.6 LSU Calibration Chamber System (Tumay and de Lima, 1992)

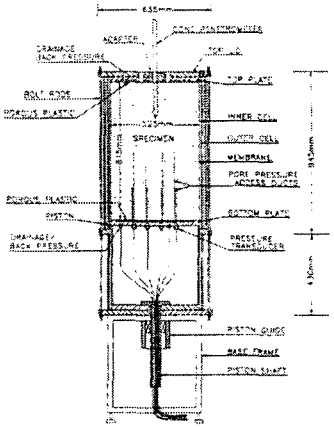

Figure 3.7 The flexible double wall chamber

3.3.2 HYDRAULIC AND CHUCKING SYSTEM

Hydraulic and push jack system allows for penetrating the cone into the sample in the chamber in one single stroke. The maximum stroke is 790 mm. This hydraulic system consists of a dual piston, and a double acting hydraulic jack mounted on a collapsible type (Figure 3.8). When the hydraulic system is extended, the full height is 2140 mm. The penetration depth is measured by the displacement transducer that works via an optical increment shaft encoder which is friction coupled to the rod (Figure 3.9).

3.3.3 DATA ACQUISITION AND MONITORING SYSTEM

The hardware of the data acquisition process consists of Gateway 2000 Pentium 200 Mhz microcomputer with 32 MB RAM, 4GB hard drive, 17 inch color monitor with 0.26 mm fine pitch CRT, a data translation DT 2801 A/D board and a digital oscilloscope (Nicolet model 310). The flow chart for data acquisition and monitoring system is depicted in Figure 3.10. A digital oscilloscope was used to capture the tip resistance and excess pore pressure of piezocone immediately after stopping penetration for the dissipation test. The general view of data acquisition system set up for calibration chamber test is shown in Figure 3.11.

Figure 3.8 Hydraulic push jack system

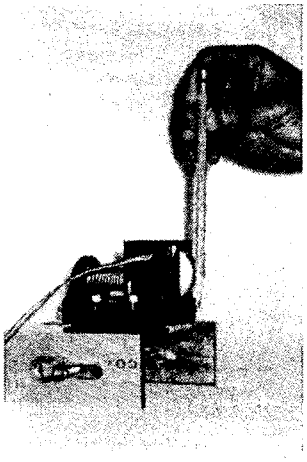

Figure 3.9 Depth encoder device

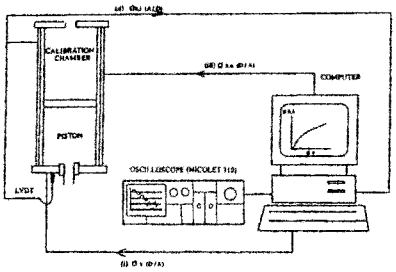

Figure 3.10 Flow chart for data acquisition and monitoring system

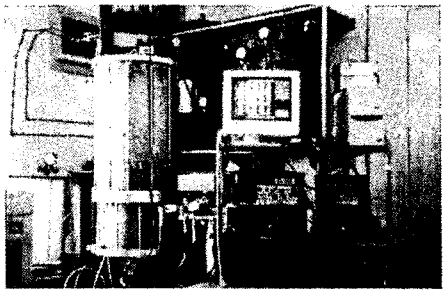

Figure 3.11 General view of data acquisition system set up

4. TEST PROCEDURE

Two main phases are used in the test procedure. They are the specimen preparation phase and the penetration phase. The stage of specimen preparation consists of two steps: slurry consolidation in consolidometer, reconsolidation in calibration chamber. Each procedure is involved with heavy instrumentation which provide detailed monitoring of the specimen environment. By using the slurry method, many of the uncertainties of field testing can be eliminated, including magnitude of in-situ stresses, stress history, and soil inhomogeneity. The technique of two stage consolidation for preparation cohesive specimens is known to produce cohesive soil specimens of very high quality (Krizek and Sheeran, 1970; Huang, et al., 1988). The triaxial pressurizing in the calibration chamber (i.e. reconsolidation) provides the stress condition of the specimen which is required for the testing scheme. The reconsolidation also reduces the rigid boundary effect resulting from first slurry consolidation stage, during which one dimensional loading was exercised with appreciable sliding of specimen along consolidometer walls.

In this study, two vertical consolidation stresses were applied to the slurry: 138 kPa, 193 kPa. The grain size distribution of the kaolin and fine sand is shown in Figure 4.1. A mixture of 33 % kaolin and 67 % Edgar fine sand by weight was used to prepare the K-33 specimen. The Atterberg limits of the virgin kaolin and K-33 mixture are shown in Table 4.1. During consolidation, pore water pressure and displacement of slurry were monitored continuously. As

an example the results of pore pressure monitored for specimen No.2 during consolidation is shown in Figure 4.2. Figure 4.3 depicts the settlement of the same specimen. The pore water pressure measurement is used to check if the real effective consolidation vertical stress is achieved. The amount of time required for full consolidation of the specimen is generally about 5.5 weeks.

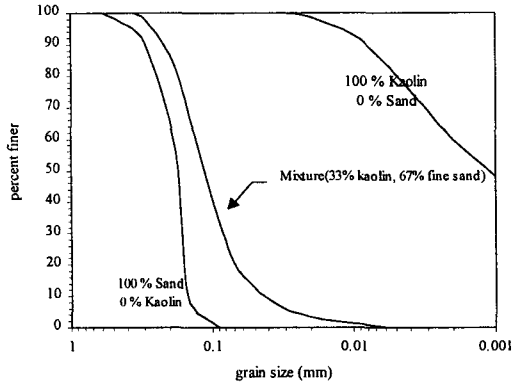

Figure 4.1 Particle size distribution curves

Soil	Liquid Limit (%)	Plastic Limit (%)	Plasticity Index (%)	Specific Gravity (G_s)
Kaolinite	54	28	26	2.66
Fine Sand	.....	.....	.....	2.67
Kaolinite and Sand (K33)	20	14	6	.....

Table 4.1 Properties of Kaolin and K-33 mixture

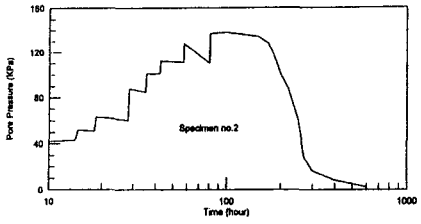

Figure 4.2 Pore pressure dissipation during slurry consolidation

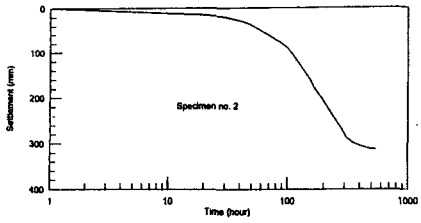

Figure 4.3 Settlement during slurry consolidation

Five specimen were prepared by the technique descrived above. For specimen 1 and 3 isotropic consolidation was applied. The stress condition of specimen 2, 4, and 5 are anisotropic and at K_0 condition (zero lateral strain). The procedure of K_0 consolidation is not as simple as the isotropic consolidation. The anisotropic K_0 consolidation followed the procedure suggested by Campanella and Vaid (1972). LSU/CALCHAS is also equipped to provide K_0 stress condition (no lateral strain) with its double flexible wall system. This system can behave as a rigid wall chamber by balancing the pressure between the inner cell and outer cell, and by maintaining constant piston pressure and preventing volume change in the cell water system. This mechanism simulates K_0 condition. Reference soil parameters are shown in Table 4.3 . These parameters were obtained from laboratory tests conducted on undisturbed samples.

4.1 PIEZOCONE PENETRATION TESTS

In this study, twenty one miniature piezocone penetration tests, and four reference piezocone tests were conducted in LSU/CALCHAS. Dissipation tests were performed at the end of all piezocone penetration tests. Prior to penetration tests, saturation (de-airing) of the filter elements was performed very carefully. The saturation of filter elements is very important to

Specimen No.	Chamber Consolidation	OCR	Final Effective Stresses (Kpa)		Lateral Stress Coefficient (K_o)
			Vertical	Horizontal	
1	Isotropic	1	207	207	1
2	Anisotropic (K_o)	1	207	86.2	0.42
3	Isotropic	1	262.2	262.2	1
4	Anisotropic (K_o)	1	262.2	104.8	0.40
5	Anisotropic (K_o)	10.9	24.2	40.71	1.70

Table 4.2 Summary of the stress history of the chamber specimens

Specimen No.	Water Content (%)	Undrained Shear Strength S_u (Kpa)	Skempton pore pressure parameter at failure, A_f	Rigidity Index $I_r = G_{50}/S_u$	Radial Coefficient of Consolidation, ($c_r \times 10^{-3}$ cm^2/sec)
1	17.36	80	0.49	100	1.9
2	19.43	85	0.37	333	4.2
3	17.22	98	0.71	167	2.2
4	17.54	121	0.25	400	4.2
5	16.80	35	-0.02	500	1.8

Table 4.3 Reference soil parameters

obtain accurate and compliant pore pressure response. The typical technique of saturation is boiling or filter elements to vacuum. All tests were conducted at the standard penetration rate of 20 mm/sec. Table 4.4 gives the summary of the cone penetration test schedule. Each penetration is identified with a Test ID which specifies pertinent characteristics about : (1) specimen number, (2) boundary condition, (3) stress condition, (4) test repetition at different location (if applicable), (5) cone penetrometer manufacturer, (6) cone type - U configuration, (7) piezocone projected area, and (8) location of penetration. The detailed legend for Test ID is given in Table 4.5.

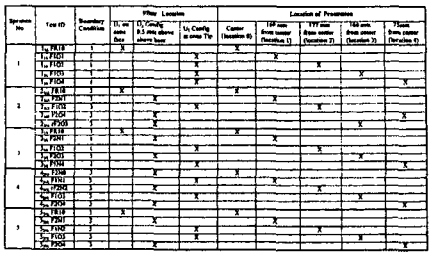

Table 4.4 Summary of the cone penetration test locations

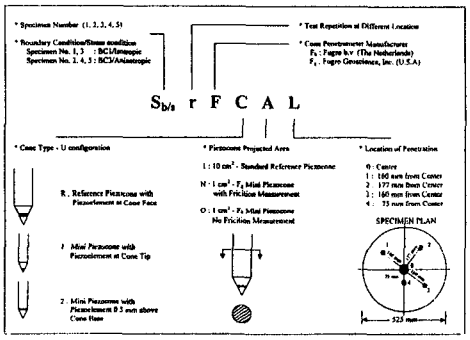

Table 4.5 Legends for Test ID

5. TEST RESULTS

The penetration testing program for this study was achieved with a total 5 large size cohesive specimens on two different stress conditions (isotropic and anisotropic, Table 4.2). In an attempt to evaluate repeatability and precision, replicate specimens were prepared. Specimen No. 1 and 3 were prepared in isotropic stress condition, and specimen No. 2, 4 and 5 in anisotropic (K0) condition. The anisotropic stress conditions specimen No. 5 was highly overconsolidated (OCR=10.9).

All specimens have a sand layer on the top of soil sample which does not reflect the true properties of the layer. The sand layer is for effective upper drainage in the stage of slurry consolidation and protection of top surface of specimen from possible damage resulting from transfer of specimen from slurry consolidometer to calibration chamber.

In the penetration profiles in specimen 1(Figure 5.1a), the steady values of corrected net tip resistance (q_T - u_0) have been obtained after reaching some depth (approximately 10cm). Although few of the excess pore pressure profiles ($u = u_T - u_0$) during the penetration exhibited poor response, in general there was a trend to approach a steady value. In the presentation of dissipation results (Figure 5.1b), the curves are plotted with normalized excess pore pressure vs. dissipation time.

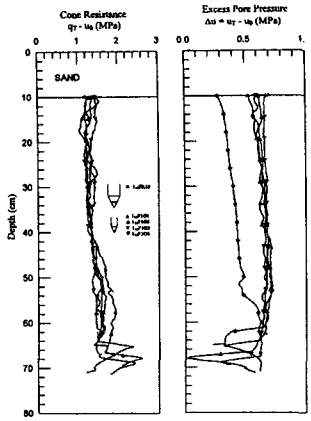

Figure 5.1a Penetration profiles in specimen 1 (See Table 4.5 for Test No. Identification)

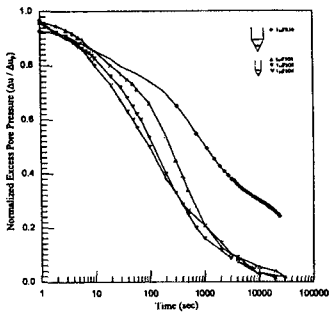

Figure 5.1b Dissipation results in specimen 1 (See Table 4.5 for Test No. Identification)

Normalized excess pore pressure is the ratio of Δu to up. Δu is the excess pore pressure ($u_T - u_0$) at the depth of interest changing with time in dissipation tests, and up is the penetration excess pore pressure ($u_p - u_0$) at the time of penetration arrest (just before stopping). From these dissipation curves, flow characteristics of specimen can be estimated. The initial starting points the curves exhibit different characteristics depending upon filter location and size of piezocone. The reason can be attributed to differences in magnitude and mode in drop of normal stress reduction that occurs when penetration ceases, and the stress redistribution that takes place around piezocone shaft after stopping penetration. Summary of the cone penetration test results and dissipation depths are given in Table 5.1

.

Specimen No.	Stress Condition	Stress History	Test	Tip Resistance, $q_T - u_0$ (Kpa)		Excess Pore Pressure, Δu (Kpa)		Dissipation Depth (cm)
				Average	Standard Deviation	Average	Standard Deviation	
1	Isotropic	OCR=1	1_{iso}FR10	1234.8	116.9	418.3	76.4	64.7
			1_{iso}F1O1	1186.1	381.5	618.5	108.1	66.5
			1_{iso}F1O2	1242.1	141.8	665.9	26.7	.....
			1_{iso}F1O3	1375.8	85.7	668.8	14.4	67.2
			1_{iso}F1O4	1192.9	138.8	643.9	33.6	61.9
2	Anisotropic (Ko)	OCR=1	2_{ani}FR10	1136.6	28.1	274.1	35.6	25.9
			2_{ani}F2N1	1182.1	11.4	.....	.....	.....
			2_{ani}F1O2	1180.7	16.6	467.0	20.0	54.2
			2_{ani}F2O4	1121.1	62.9	490.1	24.1	64.0
			2_{ani}rF2O3	1194.0	61.8	475.7	10.2	58.0
3	Isotropic	OCR=1	3_{iso}FR10	1434.7	53.1	.....	.....	57.6
			3_{iso}F2N1	1514.9	23.9	778.7	110.6	59.3
			3_{iso}F1O2	1539.9	33.8	793.6	26.3	55.4
			3_{iso}F2O3	1512.5	36.4	...	...	.....
			3_{iso}F1N4	1559.9	108.3	.....	.....	.....
4	Anisotropic (Ko)	OCR=1	4_{ani}F2N0	1406.8	23.4	517.4	27.5	51.7
			4_{ani}F1N1	1412.2	114.4	.....	.....	.....
			4_{ani}rF2N2	1329.9	91.4	527.7	36.9	55.3
			4_{ani}F1O3	1335.4	30.4	535.0	58.3	59.8
			4_{ani}F2O4	1373.3	41.4	598.3	17.5	60.1
5	Anisotropic (Ko)	OCR=10.9	5_{ani}FR10	1039.5	26.2	266.9	54.1	63.9
			5_{ani}F2N1	1067.0	17.6	243.4	57.9	51.2
			5_{ani}F1N2	1041.0	35.1	.....	.....	.....
			5_{ani}F1O3	1097.0	33.2	308.1	7.4	70.6
			5_{ani}F2O4	1077.7	29.6	288.7	10.4	55.0

Table 5.1 Summary of the cone penetration test results

5.1 RECORDING EXCESS PORE PRESSURE AND TIP RESISTANCE DURING INITIAL PHASE OF DISSIPATION USING OSCILLOSCOPE

The "initial" excess pore pressure distribution due to piezocone penetration in clays, is an important factor affecting the interpretation of the coefficient of consolidation from the piezocone test. The penetration rate changes abruptly from 2 cm/sec to 0 cm/sec when the cone is abruptly stopped for a dissipation test, resulting in a steep decrease in cone resistance accompanied by a sudden drop in the excess pore pressure around the cone path. However, this sudden drop can not be captured by using a low frequency data acquisition system. If finer data can be captured continuously (high frequency data acquisition) during penetration and instaneous halting of the probe to perform a dissipation test, it will help to investigate better the mechanism of dissipation of excess pore pressure. In order to capture this "immediate" initial drop of excess pore pressure and the simultaneous changes in tip resistance, in this research, tests have been conducted on homogeneous soil specimens and data acquired at very close time intervals (0.01 seconds) using a digital oscilloscope.

The benefit of using oscilloscope for piezocone tests is the ability of capturing fine data in extremely small time intervals. Oscilloscope (Nicolet model 310) can be set to capture 4000 data points on each sweep time. For example, if it is required to measure the tip resistance or excess pore pressure at close intervals during 40 seconds (as a sweep time) which consists of 5 seconds before and 35 seconds after stopping penetration, the oscilloscope (Nicolet model 310) may be set for capturing 100 data points each second, as depicted in the following equation:

DATA POINTS PER SECOND = 4000 / SWEEP TIME

It means one data point can be registered per 0.01 second for the example above. Oscilloscope (Nicolet model 310) consists of a display screen storage control, time per points setting part, trigger controls, and channel control. This unit captures the signal information from the cone penetrometer, converts it to digital form, and stores in magnetic disk. The data is then transferred to the main frame memory for display purposes when it is needed. All tests were triggered 5 seconds before ceasing penetration.

5.1 TEST RESULTS

Table 5.2 gives a summary of oscilloscope tests. Since the utilization of oscilloscope was adopted after specimen 2, no test results for specimen 1 are shown in Table 5.1. All tests were conducted at the standard penetration rate of 2 cm/s. The figures 5.2 and 5.3 show the change of normalized excess pore pressure ($\Delta u / \Delta u_p$) and normalized tip resistance ($\Delta q_{Tt} / \Delta q_{Tp}$) after penetration arresting. The normalization of tip resistance is based on following equation: $\Delta q_{Tt} / \Delta q_{Tp} = (q_{Tt} - u_0) / (q_{Tp} - u_0)$. q_{Tp} is the final corrected tip resistance at the time of penetration arrest. q_{Tt} is the corrected tip resistance at any time t. A sudden drop in the tip resistance was invariably observed as soon as the penetration ceased for all tests. However, the immediate change in excess pore pressures were dependent upon location of filter element and stress condition.

6. ANALYSIS OF TESTS RESULTS

The dissipation results obtained from the chamber studies were used to evaluate some of the interpretation models described earlier. The cavity expansion interpretation models proposed by *Torstensson* (1975, 1977) are compared with PCPT dissipation results of five specimens in Figures 6.1. The excess pore pressure dissipation, 0.5 mm above the cone base (for the filter element in the u_2 configuration) may not have a truly cylindrical symmetry nor a spherical one. Hence, all comparisons are made with both the cylindrical cavity expansion and the spherical cavity expansion

Specimen No.	Test	Test Depth (cm)	Stress Condition	Vertical Effective Consolidation Stress (KPa)	Ko value	Immediate Initial Drop (%)		
						Tip	Excess Pore pressure	
							U1	U2
2	$2_{3/A}$F2O4	64.0	Ko (NC)	207	0.42	14	.....	5
	$2_{3/A}$rF2O3	58.0				18	.....	2
3	$3_{1/i}$F1O2	55.4	Isotropic (NC)	262.2	1.00	18	10	.....
	$3_{1/i}$F2O3	.....				20	.....	0
4	$4_{3/A}$F2N0	51.7	Ko (NC)	262.2	0.40	13	.....	0
	$4_{3/A}$rF2N2	55.5				8	.....	0
	$4_{3/A}$F1O3	59.8				26	14	.....
	$4_{3/A}$F2O4	60.1				20	.....	0
5	$5_{3/A}$FR10	63.9	Ko (OC) (OCR=10.9)	24.2	1.70	14	11	0
	$5_{3/A}$F2N1	51.2				19	.....	0
	$5_{3/A}$F1O3	70.6				11	11	.....
	$5_{3/A}$F2O4	55.0				15	.....	0

Table 5.1 Summary of Oscilloscope Tests

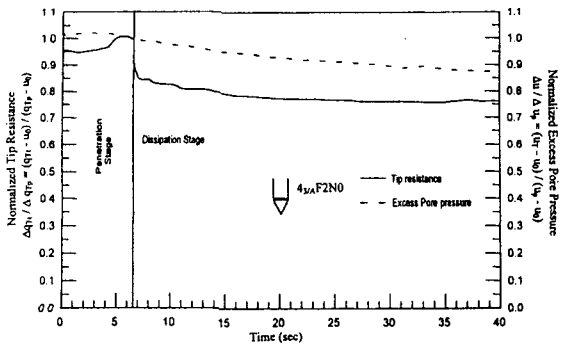

Figure 5.2 Immediate initial drop of excess pore pressure and tip resistance of $4_{3/A}$F2N0 (see Table 6.1)

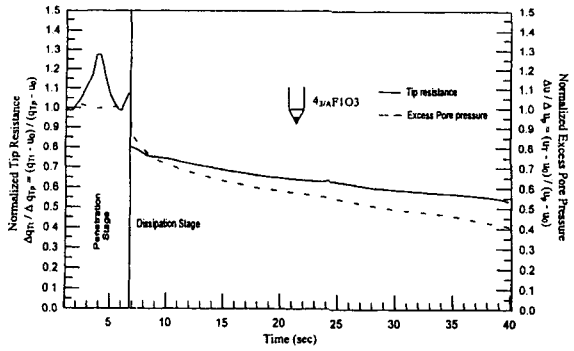

Figure 5.3 Immediate initial drop of excess pore pressure and tip resistance of $4_{3/A}$F1O3 (see Table 6.1)

solutions. It can be observed from the figures that the spherical cavity expansion solution predicts a much faster dissipation than those observed in the experiments. This is not surprising since the radius of the plastic zone (and thereby the spatial extent of the excess pore pressure distribution) predicted by the spherical cavity expansion theory is smaller than that predicted by the cylindrical cavity expansion theory. However, it is possible that during the advance of the piezocone, a deformation pattern is produced in the vicinity of the tip approximately similar to that during a spherical cavity expansion.

The limitations and disadvantages of the Torstensson's model are:

(1) Difficulty in defining the equivalent radius for the spherical cavity.
(2) Difficulty in selecting an appropriate (single) value for the rigidity index, Ir.
(3) Does not take into account the two-dimensional aspect of the cone penetration and dissipation process.
(4) Neglects shear induced excess pore pressures.
(5) It is based on a simple elastic-perfectly plastic soil model. It does not take into account geometric nonlinearities, creep effects, remolding, stress history of the soil, and coupling between total stresses and pore pressures.

However, the main advantage of the model is that it is relatively simple to use and can give an approximate estimate of cr. In general, the PCPT results obtained from the present chamber tests were in well agreement with cavity expansion solution, except specimen 5. As mentioned above, Torstenssons model can not take into account the effects of stress history and apparently is the least representative.

The theoretical solutions of Levadoux and Baligh (1986) and Houlsby and Teh (1988) using the strain path method are compared with the experimental dissipation results obtained from the chamber PCPTs in Figures 6.2. This approach was found to give unified dissipation curves for different values ofthe rigidity index, Ir. However, for any particular degree of dissipation, the difference between the time factors, T, for various filter locations cannot be a constant.

A comparison of the coefficient of consolidation cr at 50% degree of dissipation using the interpretation models are given in Table 6.3. In Table 6.3, the coefficients of consolidation cr were estimated with u_p and u_i. The u_i was defined previously as a initial excess pore pressure immediately after arresting penetration. The reference values of c_r in Table 6.3 were obtained from oedometer tests conducted on undisturbed samples obtained from chamber specimens.

The comparison between the estimated and reference values of c_r summarized in Table 6.3 reveal that utilizing u_i instead of u_p improves interpretative methods proposed by Levadoux and Baligh (1986) and Houlsby and Teh (1988) in better representing the experimental results.

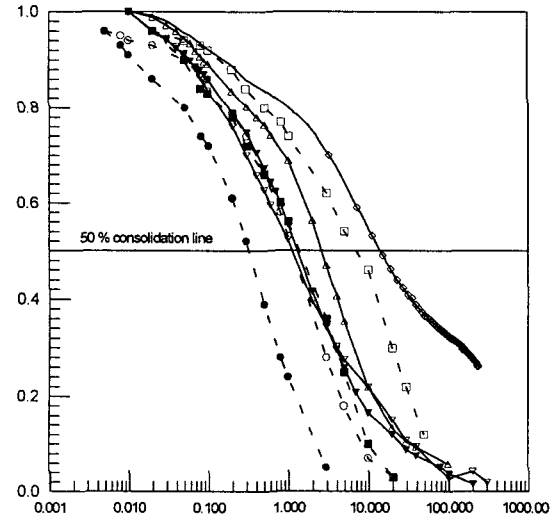

Figures 6.1 Comparison of dissipation results results in specimen 1 with the Torstenssons model

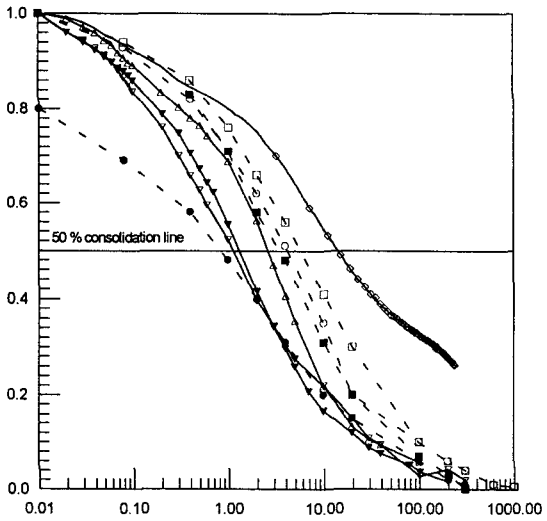

Figures 6.2 Comparison of dissipation in specimen 1 with the strain path method

Specimen No.	Test	Estimated (c_r x 10^{-3} cm^2/sec)						Reference (c_r x 10^{-3} cm^2/sec)
		Torstensson(1975,1977)		Levadoux & Baligh (1986)		Houlsby & Teh (1988)		
		With Δu_p	With Δu_i	With Δu_p	With Δu_i	With Δu_p	With Δu_i	
1	$1_{1/1}$FR10	33.8	33.8	7.8	7.8	2.5	2.5	1.9
	$1_{1/1}$F101	3.4	3.4	4.1	4.1	1.0	1.0	
	$1_{1/1}$F103	3.1	3.1	10.5	10.5	2.0	2.0	
	$1_{1/1}$F104	3.7	3.7	9.7	9.7	2.0	2.0	
2	$2_{3/A}$FR10	31.7	31.7	1.2	1.2	1.0	1.0	4.2
	$2_{3/A}$F102	3.4	3.7	33.1	2.7	11.3	9.3	
	$2_{3/A}$rF203	4.0	3.7	16.0	13.7	12.7	5.3	
	$2_{3/A}$F204	2.7	3.9	13.5	16.9	10.8	6.5	
3	$3_{1/1}$F2N1	3.1	3.3	8.8	6.8	5.0	1.9	2.2
	$3_{1/1}$F102	3.4	3.5	44.6	33.6	10.7	8.1	
4	$4_{3/A}$F2N0	3.1	3.5	2.9	3.2	2.6	1.3	4.2
	$4_{3/A}$rF2N2	3.1	3.3	2.2	2.3	2.0	1.0	
	$4_{3/A}$F103	3.5	3.3	29.0	20.6	11.0	7.7	
	$4_{3/A}$F204	3.3	3.9	11.7	12.7	10.2	5.3	

*** Specimen 5 was excluded since all interpretation models are valid only for OCR5

Table 6.1 Comparison between the estimated and reference cr values at 50 % dissipation level

7. CONCLUSIONS

(1) The two stage slurry consolidation technique was successfully used to prepare large size cohesive soil specimens of known stress histories for calibration chamber testing. The specimens prepared were reproducible and homogeneous as was indicated by the settlement and pore pressure dissipation histories and by the water content results obtained from samples taken from the chamber specimens. The homogeneity of the specimens was additionally confirmed by the cone penetration results (q_T, Δu profiles) in each specimen.

(2) For specimen 1 and 3 the isotropic consolidation was applied, and specimens 2, 4, and 5 were subjected to anisotropic K_0 reconsolidation. The procedure of anisotropic K_0 reconsolidation is not as simple as isotropic consolidation. The performance of the reconsolidation followed the One increment (or Single increment) procedure suggested by Campanella and Vaid (1972). Campanella and Vaid utilized a rigid wall chamber to eliminate lateral strain. LSU/CALCHAS used in this research eliminates lateral strain (K_0 condition) with its servo-controlled double flexible wall system.

(3) In order to capture the immediate excess pore pressure drop and the simultaneous changes in cone tip resistance penetration data was acquired at very close time interval (0.01 seconds) using a digital oscilloscope.

(4) High frequency data acquisition using a digital oscilloscope clearly indicated sudden drops in the corrected tip resistance, and substantial changes in the tip excess pore pressure (u1 type filter), when the penetration was arrested to conduct dissipation tests. This is primarily due to the normal stress reduction at the tip, as the penetration rate changes abruptly from 2 cm/s to 0 cm/s. Dissipation and pore pressure redistribution around the tip could also contribute to this effect. The u_2 type filter located just above the cone base, barely showed any instantaneous excess pore pressure drop. This is because of the fact that above the cone base there is a normal stress release, and the excess pore pressures are predominantly induced by shear (compared to excess pore pressure at the cone tip, which are primarily dominated by octahedral normal stresses).

(5) Comparison between the estimated and reference values of c_r reveal that utilizing the initial excess pore pressure values immediately after the sudden drop (u_i) instead of the penetration excess pore pressure (u_p) improve the interpretative methods proposed by Levadoux and Baligh (1986), and Houlsby and Teh (1988) in better simulating experimental results.

8. REFERENCES

1. Acar, Y. B. and Tumay, M. T., 1986, "Strain Field around Cones in Steady Penetration," Journalof Geotechnical Engineering, Vol. 112, No. GT2, pp. 207-213.1.
2. Baligh, M. M. and Levadoux, J. N., 1986, "Consolidation After Undrained Piezocone Penetration. II: Interpretation," ASCE, JGED, Vol. 112, No. 7, pp. 727-744.2.
3. Campanella, R. G. And Vaid, V. P., 1972, A simple Ko Triaxial cell, Canadian Geotechnical Journal, Vol. 9, pp. 249.
4. de Lima, D. C., 1990, "Development, Fabrication and Verification of the LSU In Situ Testing Calibration Chamber," Ph.D. Dissertation, Louisiana State University, Baton Rouge, LA, 340 p.
5. Houlsby, G. and Teh, C. I., 1988, "Analysis of the Piezocone in Clay," ISOPT I, Orlando, Florida, Proceedings, Vol. 2, pp. 777-783.5.
6. Huang, A. B., Holtz, R. D. and Chameau, J. L., 1988, "A Calibration Chamber for Cohesive Soils," ASTM Geotechnical Testing Journal, Vol. 11, No. 1, pp. 30-35
7. Kurup, P. U. And Tumay, M. T. Piezocone Dissipation Curves with Initial Excess Pore Pressure Variation, Proceedings, International Symposium on Cone Penetration Testing, CPT95, Linkoping, Sweden, October 1995, pp. 195-200.
8. Kurup, P.U., Voyiadjis, G. Z. And Tumay, M. T., Calibration Chamber Strudies of Piezocone Tests in Cohesive Soils, Closure, ASCE, Journal of Geotechnical Engineering Division, Vol. 121, No. 5, May 1995, pp. 455-456.
9. Teh, C. I. and Houlsby, G. T., 1991, "An Analytical Study of the Cone Penetrometer Test in Clay," Geotechnique, Vol. 41, No. 1, pp. 17-34.
10. Tumay, M. T. and Acar, Y. B., 1985, "Piezocone Penetration Testing in Soft Cohesive Soils," Strength Testing of Marine Sediments: Laboratory and In-Situ Measurements, ASTM STP 883, American Society for Testing and Materials, Philadelphia, PA, pp. 72-83.
11. Tumay, M. T. and de Lima, D. C., 1992, "Calibration and Implementation of Miniature Electric Cone Penetrometer and Development, Fabrication and Verification of the LSU In-situ Testing Calibration Chamber (LSU/CALCHAS)," LTRC/FHWA Report No. GE-92/08, 240 pp.
12. Tumay, M.T., Kurup, P.U., and Voyiadjis, G. Z., Profiling Lateral Stress Coefficient and Overconsolidation Ratio from Piezocone Penetration Tests, Porceedings, International Symposium on Cone Penetration Testing, CPT95, Linkoping, Sweden, October 1995, pp. 337-342.